NOMAD Collaboration

NOMAD/MEMO 2000-06
October 1, 2000

STAR Noise and Hit-Finding Efficiency

J. Kokkonen, F.J.P. Soler, G. Vidal Sitjes

CERN

Abstract

The first part of this note describes the STAR noise. This includes descriptions of the production of the noise and the long-term behaviour of the noise. A justification for the use of day-by-day noise files is provided. The second part discusses the hit-finding efficiency, including a method for the maximisation of the hit-finding efficiency by varying the cuts used in the hit-finding on a ladder-by-ladder basis. The reasons for the differences in efficiciencies are also investigated.

1 Introduction

The primary aim of this work has been to provide the correct noise information of STAR for the reconstruction and to optimise the hit-finding efficiency. In addition, an effort has been made to understand the noise behaviour and the reasons for the variations in the efficiency in this prototype detector. The results herein apply to the 1998 run, which provides most of the STAR data.

This memo is organised as follows. Section 2 begins with a discussion of the on-line pedestal subtraction. This is followed by a description of the noise production algorithm. Finally, a detailed study of the noise behaviour is done. In addition to providing a deeper understanding of the detector, it provides the justification for the approach taken in the noise production. In Section 3 the hit-finding procedure is presented first. Next, the method for the efficiency calculation and the maximisation of the efficiency through the optimisation of the hit-finding cuts is discussed. This is followed by the results of the optimisation in terms of the hit-finding efficiency and the hit-finding cuts used to obtain the efficiencies. Finally, findings from laboratory measurements made after the neutrino runs are presented. The findings explain some of the performance differences of the ladders. The final section presents the conclusions.

2 Noise

2.1 Pedestals

The numbering scheme adhered to in this memo is the following. The planes are numbered 1-5 with plane 1 furthest upstream and plane 5 next to the drift chambers. Each layer contains 10 ladders, ladder 1 being the bottom-most ladder, and 5 electronics chips per ladder, chip 1 being the bottom-most. Although each chip has 128 channels, all the 640 channels on a ladder are numbered consecutively, again with channel 1 at the bottom.

The pedestals are the average read-out values of the channels when there is no signal. This base-level on the channels is typically of the order of a few hundred ADC counts. The pedestal file for a run is made using data from the previous run. The data is taken during the calibration cycle of the beam, i.e. during the approximately 12 s of no beam of the full 14.4 s cycle. Of the order of 10-20 calibration events are recorded using pulsed triggers during each calibration cycle. In order to make the pedestal file for the following run, 2600 pedestal calibration events are required. If the statistics are insufficient at the end of a run, the pedestals taken thus far are kept until there are enough pedestal events to make a new pedestal file. This is to avoid the potential problem of using an old pedestal file, which could happen if the runs were too short to record enough pedestal events.

The data is always stored and used in the pedestal-subtracted form and on a channel-by-channel basis. Therefore the read-out values of the channels are centered around zero in the absence of signal. The pedestals are distinct for each ladder and were found to be very stable. An example of the pedestals for a ladder is shown in Fig. 1.

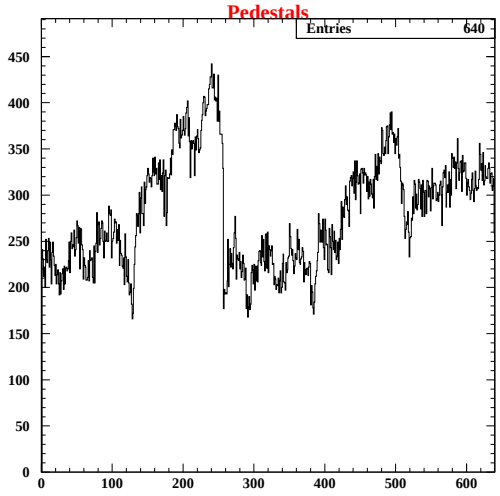

Figure 1: The pedestals for the 640 channels of ladder 1 on plane 1. A channel-by-channel approach is used and the pedestals are recalculated for every run.

2.2 Noise production

The noise is calculated completely independently from the procedure for pedestals. It is done off-line on a day-by-day basis using data from muon events. The noise is defined as the RMS fluctuation of the read-out signal value around the base value, or pedestal, after common-mode noise (CMN) subtraction when there is no true signal. The noise is measured in units of ADC counts, with 1 ADC count corresponding to approximately 250 e^-.

For each event used to calculate the noise, the CMN has to be established first. The CMN is the average, or common, jump in the signal-level for all 128 channels on a chip for an event. The CMN is due to a common pick-up of noise for all the channels on a chip in a particular event.

The event-by-event CMN subtraction is done according to the following procedure for each chip:

- the CMN per chip is calculated,
- the RMS deviation around the CMN for all channels on the chip is calculated,
- only those channels for which the RMS deviation around the CMN is between 0.9 and 25 are used,
- the CMN per chip is recalculated, including only those channels which have a signal value within three times the RMS from the chip mean,
- the CMN value is subtracted from the read-out signal value for all channels on the chip.

Once the CMN subtraction has been done, calculating the RMS noise using the muon events is straight-forward. This is done in a new iteration, in which the events for which the read-out value

is not within three times the RMS of the corresponding strip are excluded. This is so that hits due to muons are not inadvertently included in the noise calculations.

The procedure outlined above results in day-by-day noise files for each of the 32000 channels, with the number of muon events per day used for these calculations ranging from approximately one hundred to a few thousand. The full 1998 neutrino run consists of 171 days. There are gaps for those days in which there was no data, mainly due to the servicing of NOMAD (7 out of 171 days).

2.3 Noise behaviour

The noise behaviour of STAR throughout the 1998 data-taking period was studied extensively. The motivation for this was three-fold:

- to understand the detector better,
- to verify the validity of the noise files and to show that day-by-day noise files are justified,
- to attempt to understand the low efficiency of some ladders and to attempt to rectify possible problems off-line.

The full sample of 164 daily noise files over the 171 day data-taking period, from 2 April to 19 September, was used to study the noise with the exception of two days. One had low statistics (under 100 muon events) and the other had abnormally high noise values which are thought to be due to an error. As studying the noise of 32000 individual channels is impractical, the noise was mainly studied at the chip level. The chip noise was defined as $\sqrt{\frac{\sum_{i=1}^{128} N_i^2}{128}}$, where N_i is the noise of the ith strip on the chip.

Most chips exhibit very stable noise behaviour throughout the year, with the noise remaining constant throughout the year at approximately 6 ADC counts. An example is shown in Fig. 2, showing the day-by-day noise. Days 1-29 correspond to April, 30-60 to May, 61-90 to June, 91-121 to July, 122-152 to August and 153-171 to September.

Some chips show unstable noise behaviour and are characterized by periods in which the noise increases gradually from the base-level to level-out at a higher noise value, to suddenly being reset to its original base-level. This resetting coincides with the detector being switched off, typically for a few days. This happens for example for scheduled service interventions of NOMAD or the beam and usually last 1-2 days. It should be noted that at approximately day 140, the detector is only switched off for 7 hours and the noise-level is not completely reset. This suggests that the detector resets gradually after being switched off.

All unstable chips show the same general behaviour and three distinct periods can be identified. In April, the noise is fairly stable with only a slight increase. In May and up to mid-June, there is a period of steady increase in the noise. From mid-June the increase in the noise is more pronounced.

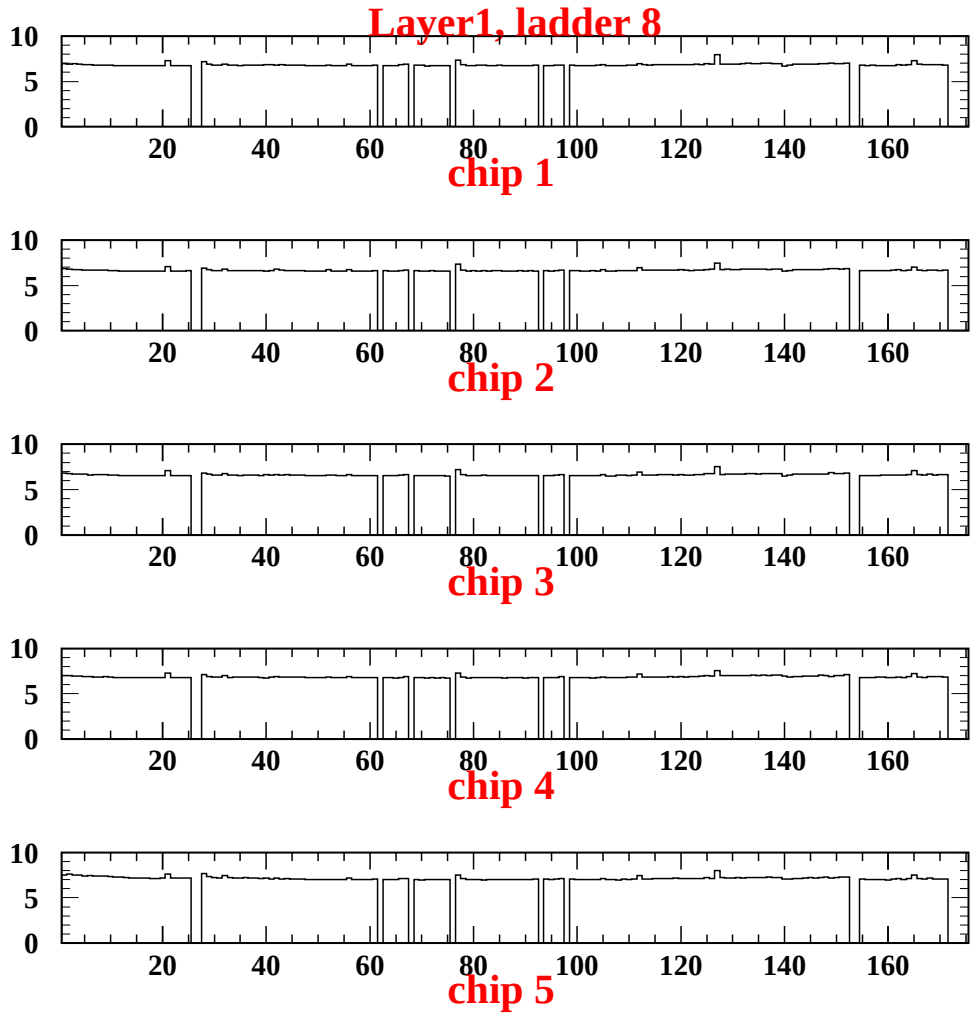

Figure 2: Chip noise evolution in time. The horizontal axis represents the days in the 1998 run from April to September. The vertical axis shows the RMS ADC noise count for the chip. The gaps correspond to days with no data.

However, the noise plateaus out within 20 days to a new level. An example is shown in Fig. 3. One can also conclude that the changes from day-to-day are small and that daily noise files are adequate.

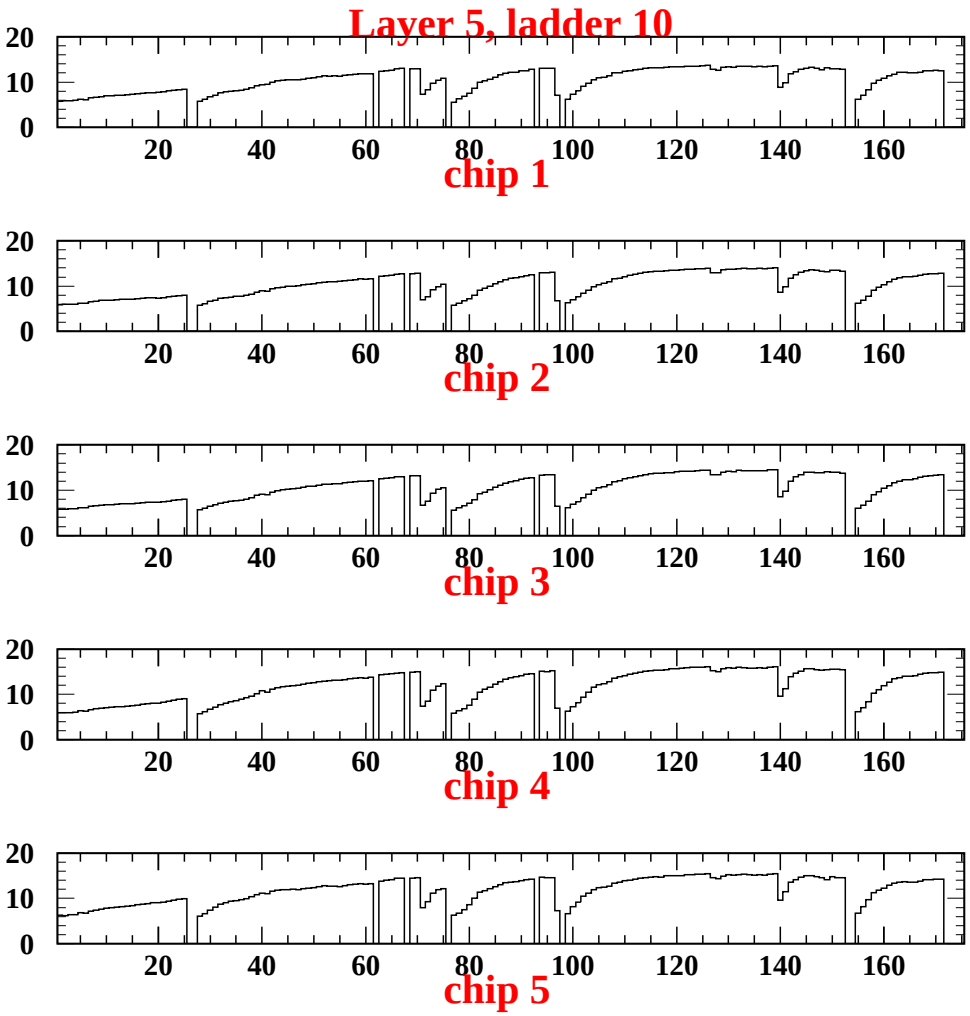

Figure 3: Noise evolution for unstable chips for April through to September.

It is interesting to note that all the chips from a ladder show mutually similar behaviour, apart from small peaks and ripples. This means that the general noise behaviour can be determined at the ladder level. However, ladders connected to the same repeater card do not necessarily show similar behaviour. Chips on 13 ladders, about a quarter of the total, show the unstable noise behaviour clearly, although chips on up to a dozen further ladders show some signs of this.

Finally, to justify the chip-by-chip or ladder-by-ladder approach, it should be noted that individual channels show behaviour similar to the overall behaviour of the chip and hence the ladder. Fig. 4 shows an example of the noise behaviour of individual strips from the same ladder displayed in Fig. 2.

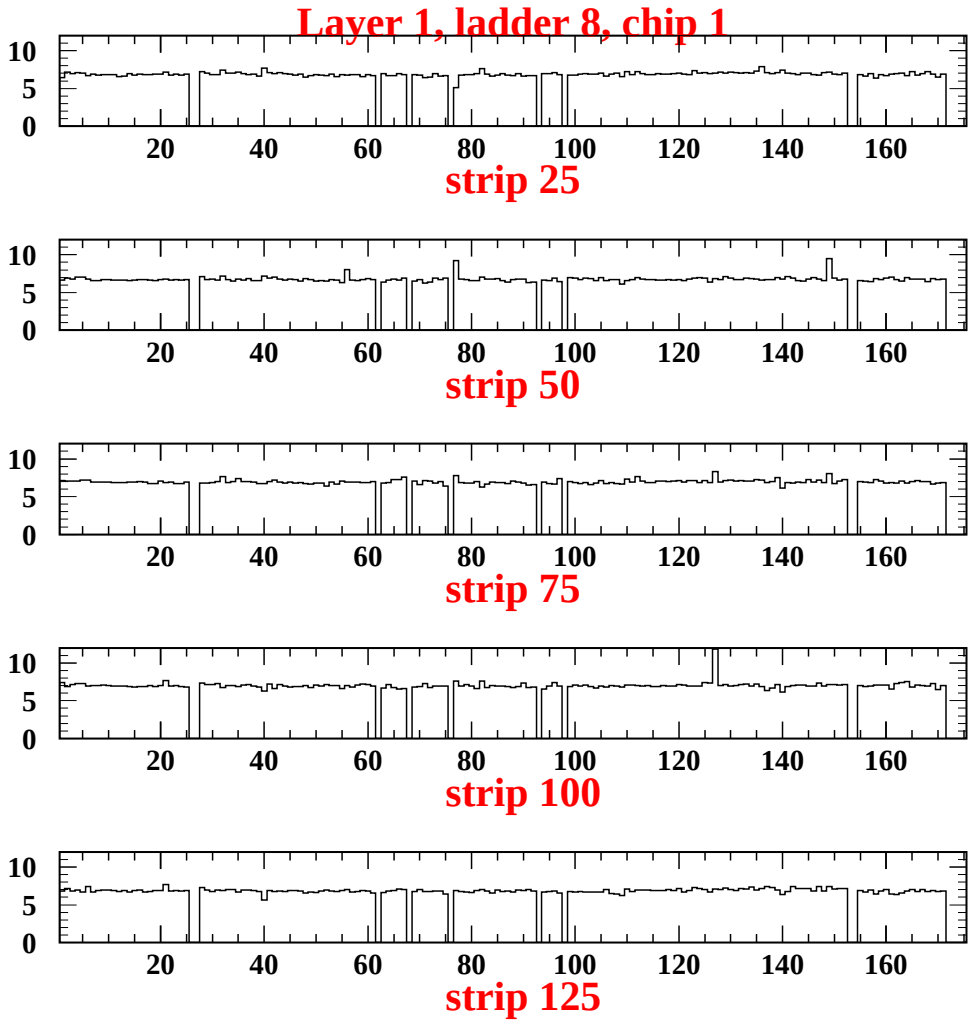

Figure 4: Noise evolution in time for individual channels.

The distribution of noise for all the channels of the whole detector on a typical day at the start of the run is shown in Fig. 5. Distributions for later days are similar although sometimes slightly wider.

The distribution of RMS chip noise for the whole year is shown in Fig. 6. The noise distribution is centered around 6 ADC counts, with the full-width-half maximum value at approximately 1 count. However, 49 chips have an average noise greater than 8 ADC counts. These all correspond to unstable chips as only the unstable chips exhibit high noise. Finally, the ladder-by-ladder noise is shown in Fig. 7 to identify which ladders have high noise. It should be noted that layers 3 and 4 in particular have high-noise ladders, along with ladder 10 of plane 5.

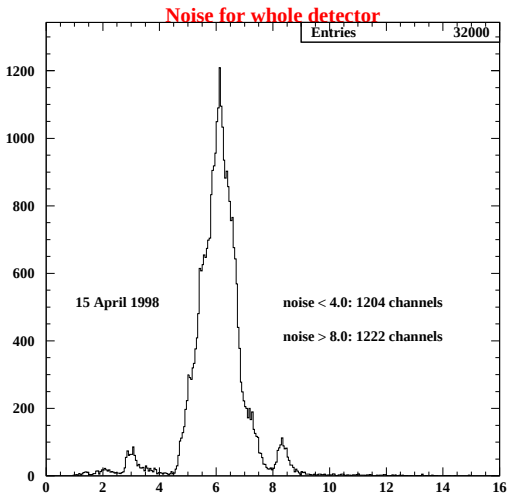

Figure 5: Noise distribtion for a day at the start of the run.

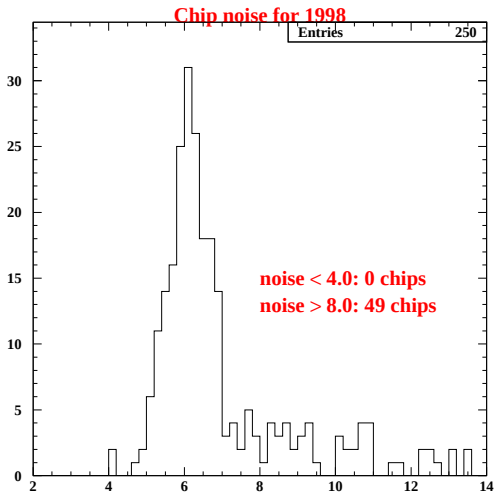

Figure 6: The distribution of average chip noise for 1998.

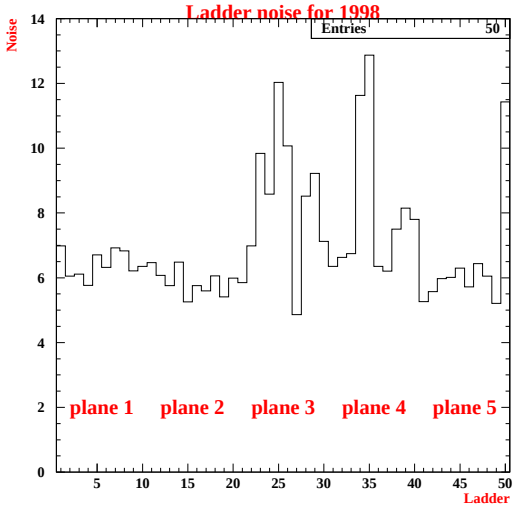

Figure 7: The average noise for 1998 shown ladder-by-ladder.

3 Hit-finding efficiency

3.1 Hit-finding

When a charged particle traverses the detector, most of the charge is shared among the two closest strips, a readout strip and a floating strip. The rest of the charge is shared among neighboring strips due to capacitive coupling, as described in [1]. The readout strip that has the highest charge is called the seed strip while collectively the strips sharing the charge are called the cluster. Hits are identified based on the following signal-to-noise ratio (S/N) criteria:

- a cut on the S/N of the seed strip: the seed cut,
- a cut on the S/N of the neighboring strips: the neighbor cut,
- a cut on the sum of the S/N of the strips included in the cluster, according to $(S/N)_{cluster} = (S/N)_{seed} + \sum_i (S/N)_{seed-i} + \sum_i (S/N)_{seed+i}$: the cluster cut.

The following algorithm is used when forming clusters to identify hits:

- all strips with a S/N above the seed cut are sorted in order of decreasing S/N,
- seed strips are required to be separated by at least two strips; if not, seed strips with lower S/N are not considered,
- starting from the seed strip with the highest S/N, a maximum of three consecutive strips on either side of the seed strip are included in the cluster until a strip does not pass the neighbor cut or it has already been taken by another cluster,

- finally the cluster is required to pass the cluster cut.

The final hit-position is determined by the model in [1], taking into account the interstrip and backplane capacitances.

3.2 Calculating the hit-finding efficiency

The efficiency studies are performed using reconstructed muon events. To ensure adequate statistics, the efficiencies are calculated ladder-by-ladder. As each ladder consists of 12 individual silicon detectors which are bonded together, there is a gap in the active region between each of these detectors. Therefore, for the purposes of the efficiency study, only tracks which pass through the active regions of each plane are used. In fact only the central 2.2 cm of the 3.2 cm active width of the individual silicon detectors is used. The tracks are also required to pass through the same corresponding ladder of each layer, e.g. the 3rd ladder of each layer. This implies that the muon tracks should be straight. The relationship between the angle of muon tracks in STAR and the momentum of the muons is shown in [5]. To avoid high-angle tracks and to minimise the multiple scattering angle, only muons above 10 GeV momentum are selected for the efficiency study. An unusual muon run from mid-July to mid-August, consisting of a highly collimated and energetic beam, was not used.

The muon track is reconstructed in the standard way with a hit required in each of the four ladders which are not under study. For example, if the 3rd ladder of the 1st plane is under study, a hit is required in the 3rd ladder of planes 2, 3, 4 and 5. The area within 1 mm of the extrapolated (or interpolated) hit position of the muon track to the ladder under study is considered for hits. The overall efficiency is defined as the ratio of the number of times at least one hit is found to the total number of muon tracks considered. For the single-hit efficiency, exactly one hit (or, equivalently, one cluster) is required within the 1 mm roadwidth. When considering single-hit efficiency, those cases which have two or more hits within the roadwidth are not allowed. This serves the purpose of limiting the number of times a so-called ghost hit is mistakenly used for efficiency calculations.

Initially, all the ladders were given the same seed, neighbor and cluster cuts, as discussed in [1]. However, preliminary efficiency studies [2], [3] showed considerable differences between ladders, suggesting the cuts should be optimised. Preliminary work in cut optimisation are presented in [4]. Due to limited statistics and the assumption that all the chips on the same ladder perform in a similar manner, it was decided to optimise the cuts ladder-by-ladder.

3.3 Hit-finding efficiency

The efficiency is maximised by optimising the S/N cuts. This is done by first maximising the single-hit efficiency for the seed cut, while setting the neighbor cut to 0.5 and ignoring the cluster cut. This means that for every ladder, the seed cut was optimised so that the efficiency to find exactly one strip passing the seed cut within the 1 mm roadwidth was maximised. Next, the seed cut and the fixed neighbor cut of 0.5 are retained and the efficiency is maximised by varying the

cluster cut. This results in seed cuts for the ladders which vary from 3.4 to 4.4, with a median value of 3.9 while the cluster cut varies from 3.8 to 6.1, with a median value of 4.8, as shown in Fig. 8. The cluster cut of ladder 5, plane 2, is lower than the seed cut, a consequence of the optimisation algorithm, indicating that for this ladder the cluster cut plays no role. The seed and cluster cuts are shown by ladder in Fig. 9 and Table 1. By comparing to Section 1, one sees that there appears to be a weak inverse correlation between the ladder noise and seed cut.

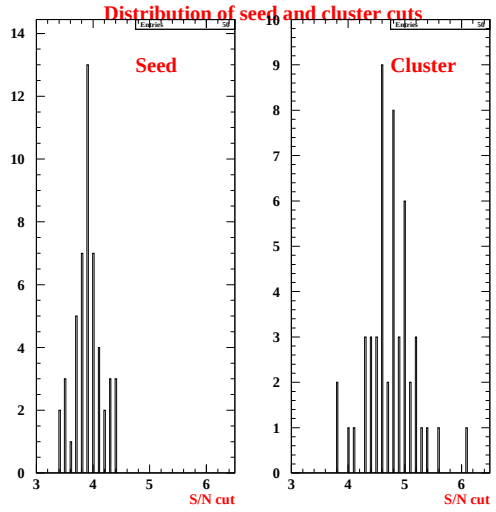

Figure 8: The distribution of the seed and cluster cuts for all ladders.

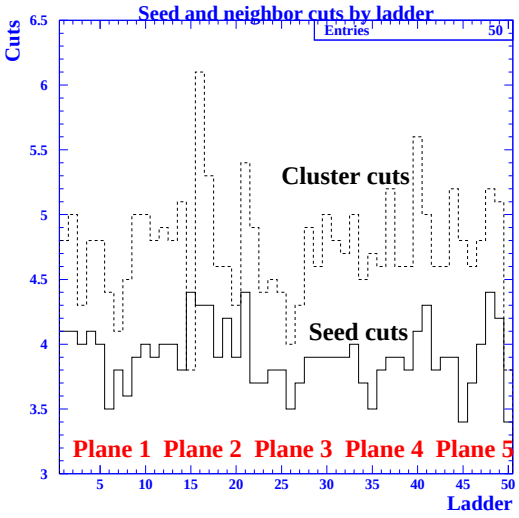

Figure 9: The seed and cluster cuts by ladder. The solid line corresponds to the seed cut and the dashed line to the cluster cut.

The overall efficiency resulting from the optimised cuts is shown in Fig. 10. Planes 2 and 3 attain a level of nearly 100%, with plane 1 nearly at this level. The performance of the ladders in planes 4 and 5 is somewhat worse, even dropping below 95 %. It is not surprising that plane 1 does not

ladder/plane	1	2	3	4	5
1	4.1/4.8	3.9/4.8	4.4/5.4	3.9/4.8	4.3/5.0
2	4.1/5.0	4.0/4.9	3.7/4.9	3.9/4.7	3.8/4.6
3	4.0/4.3	4.0/4.8	3.7/4.4	4.0/5.0	3.9/4.6
4	4.1/4.8	3.8/5.1	3.8/4.5	3.7/4.5	3.9/5.2
5	4.0/4.8	4.4/3.8	3.8/4.4	3.5/4.7	3.4/4.8
6	3.5/4.4	4.3/6.1	3.5/4.0	3.8/4.6	3.7/4.6
7	3.8/4.1	4.3/5.3	3.7/4.3	3.9/5.2	4.0/4.8
8	3.6/4.5	3.9/4.6	3.9/4.9	3.9/4.6	4.4/5.2
9	3.9/5.0	4.2/4.6	3.9/4.6	3.8/4.6	4.2/5.1
10	4.0/5.0	3.9/4.3	3.9/5.0	4.1/5.6	3.4/3.8

Table 1: The seed and cluster cuts for the ladders.

show optimum performance as this is where the *a priori* poorest ladders were placed during the construction. The poor performance of ladders 4 and 5 can be traced to calibration errors of the electronics, as discussed in the next section.

As a comparison, the overall efficiency is also shown with all ladders using fixed cuts of 4.0, 0.5 and 7.5, for the seed, neighbor and cluster cuts, respectively. The efficiencies are considerably lower, and more importantly, there is considerable fluctuation. The fluctuation suggests different gains of the amplifiers on the ladder, justifying the approach of optimizing the cuts ladder-by-ladder.

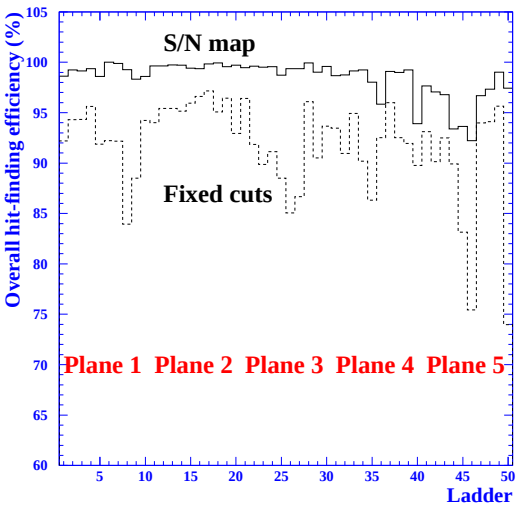

Figure 10: The overall hit-finding efficiency by ladder for optimised and fixed S/N cuts. The solid line corresponds to the optimised cuts and the dashed line to fixed cuts.

The overall hit-finding efficiency, shown in Fig. 10, is also shown in Table 2, along with the statistical error. The error, obtained by assuming binomial statistics, is given by $\frac{1}{N}\sqrt{\frac{n(N-n)}{N}}$, where n is the

number of hits in the ladder counting for the efficiency and N the total number of events used to obtain the efficiency. However, if $n = N$, the error is calculated using $1/N$, as is the case for ladder 6 of plane 1. The higher statistical errors of ladders 5, 6 and 10 of each plane are in part due to the lower number of events for these ladders.

ladder/plane	1	2	3	4	5
1	98.6±0.2	99.6±0.1	99.5±0.1	98.7±0.2	97.7±0.2
2	99.2±0.1	99.6±0.1	99.6±0.1	98.8±0.2	97.1±0.2
3	99.1±0.1	99.7±0.1	99.5±0.1	99.1±0.1	96.8±0.3
4	99.4±0.1	99.7±0.1	99.6±0.1	99.2±0.1	93.4±0.4
5	98.6±0.3	99.4±0.2	98.7±0.3	98.0±0.4	93.6±0.6
6	100.0±0.1	99.4±0.3	99.4±0.3	95.9±0.6	92.2±0.8
7	99.9±0.1	99.8±0.1	99.4±0.1	99.1±0.2	96.7±0.3
8	99.3±0.1	99.9±0.04	99.9±0.04	99.0±0.2	97.3±0.3
9	98.3±0.2	99.6±0.1	99.0±0.2	99.2±0.2	99.0±0.2
10	98.6±0.4	99.7±0.2	99.6±0.2	93.9±0.7	97.4±0.5

Table 2: The overall hit-finding efficiency and statistical error (%) for the ladders.

The single-hit efficiencies using the optimised cuts are shown month-by-month in Fig. 11, with July and August combined due to the low number of muon events. Although there are variations from month-to-month, the general levels remain the same, suggesting that cuts varying in time are not necessary.

3.4 Hit-finding efficiency in the laboratory

Planes 1 and 5 were investigated in the laboratory after the 1998 run to see whether the losses in efficiency were due to the ladders themselves or due to the electronics. The ladders were tested individually, sandwiched between a pair of scintillators for triggering, using a Ru-source. A hit in the ladder was recorded for a seed cut of 5.0, with no neighbor or cluster cuts used. The efficiency was defined as the ratio of the number of hits in the ladder to the total number of triggers.

The ladders were tested with the same repeater card they were connected to in STAR and also with one optimised in the laboratory. The repeater card contains the amplifying and shaping circuitry, although the pre-amplifiers are on the ladders themselves. The results are shown in Fig. 12.

For plane 1 the efficiencies with the optimised electronics are slightly better than with their own electronics. This suggests that a slight advantage could have been gained by fine-tuning the electronics. However, as both sets of electronics give comparable results yet some of the efficiencies are low, it is clear that part of the performance degradation is due to the ladders themselves. It should be noted that poor performance is shown for ladder 5 in the laboratory measurements. As this poor performance is not seen in the off-line efficiency studies, the low efficiency is presumed to be due to a failure of the ladder occuring after the 1998 run, for example due to mishandling of

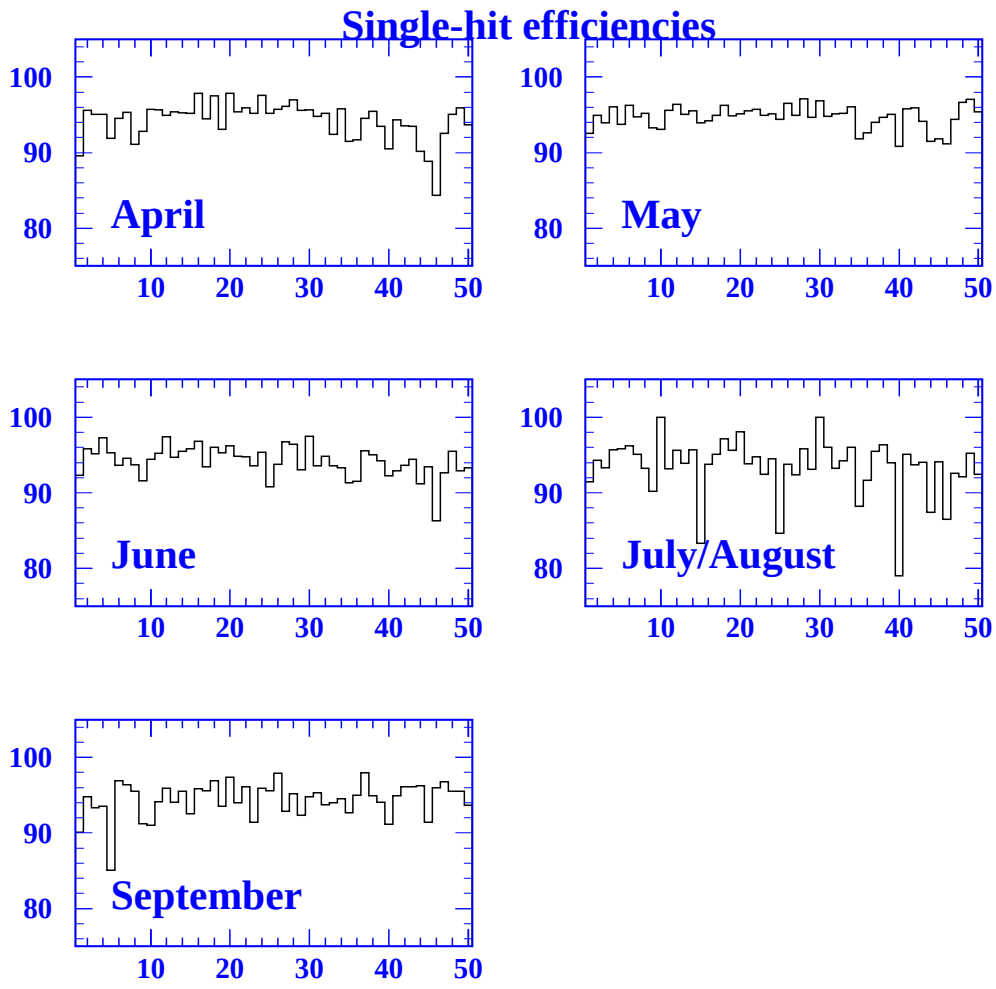

Figure 11: The monthly single-hit efficiencies by ladder for optimised S/N cuts.

the ladder.

For plane 5 there is a dramatic drop in efficiency for ladders 5, 6 and 10 when using their own electronics compared to the optimised electronics. Further investigation of the settings of the corresponding repeater cards showed that they had been incorrectly calibrated. We presume that the low efficiencies in plane 4 are due to the same reason. It should be noted that when using the optimised electronics with plane 5, the measured efficiencies are over 90% and thus higher than the efficiencies for plane 1. This strongly suggests that the ladders themselves in plane 5 perform very well.

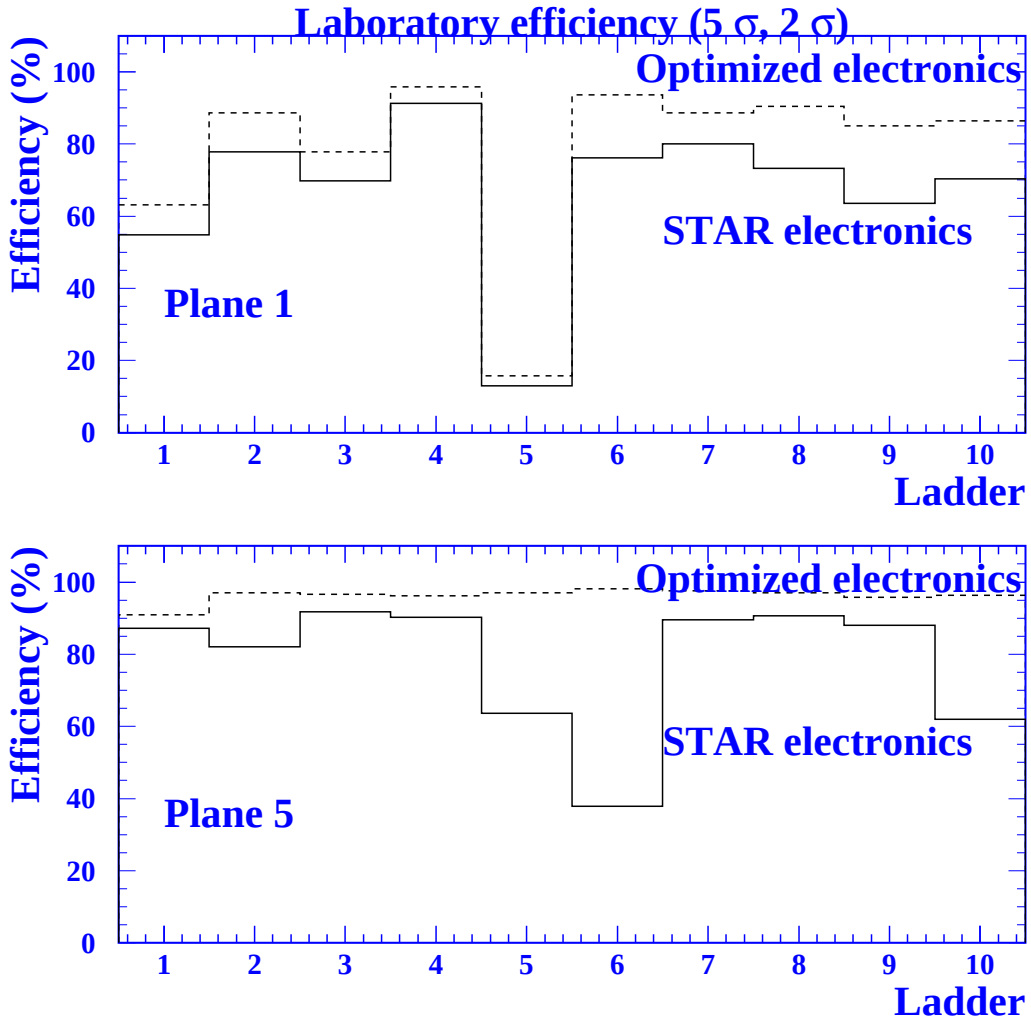

Figure 12: Ladder efficiencies in the laboratory for planes 1 and 5.

4 Conclusion

The pedestal and noise behaviour of the detector are well understood. The pedestals are stable and are calculated on-line on a channel-by-channel basis. Usually a new pedestal file is created for every run. The noise is calculated off-line, also on a channel-by-channel basis, independently from the pedestals. It was found that although most ladders have stable noise, some ladders show long-term unstable noise behaviour. However, the noise value is reset to its original value when the detector is switched off. As the noise does not change significantly from one day to the next, calculating the noise on a daily basis is adequate.

The measurement during data-taking using muons and in the laboratory clearly show that some ladders have a degraded hit-finding efficiency, although most ladders perform well. This seems to arise mainly from low gain due to incorrectly calibrated repeater cards, as shown by measurements in the laboratory after the run. The noise is not found to have a significant effect on the efficiencies. Most of the hit-finding efficiency is recovered by optimising the S/N-cuts on a ladder-by-ladder basis.

Acknowledgements

We are indebted to all those contributing to STAR through their time and effort. In particular our thanks go out to A. Cervera-Villanueva, E. do Couto e Silva, M. Ellis, D. Ferrère, J.J. Gomez-Cadenas, M. Gounaère, J.A. Hernando, V.E. Kuznetsov, L. Linssen, O. Runolfsson, G. Baricchello, D.C. Daniels, L. Camilleri, L. Dumps, C. Gößling, S. Geppert Soulie, W. Huta, J.M. Jimènez, B. Lisowski, J. Long, A. Lupi, K. Mühlemann, J. Mulon, B. Schmidt, D. Steele, M. Stipčević, M.Veltri and D. Voillat. We would also like to acknowledge summer students J. Pinney and M. Smedbäck, who did important groundwork for the efficiencies. Finally, we thank the NOMAD institutions for their encouragement and support.

References

[1] *Performance of Long Modules of Silicon Microstrip Detectors*, G. Baricchello *et al.*, Nuclear Instruments and Methods Phys. Res. A 413 (1998) 17-30.

[2] *Primary vertex reconstruction for the silicon ladders of NOMAD-STAR and a laboratory test system for silicon detectors*, J. Pinney, NOMAD-MEMO/98-018 (1998).

[3] *Studies on hit finding efficiencies for the silicon ladders of NOMAD-STAR*, G. Vidal Sitjes, NOMAD-MEMO/98-019 (1998).

[4] *Examination of efficiency of the Nomad Star detector for matching of detector hits and reconstructed tracks*, M. Smedbäck, NOMAD-MEMO/99-011 (1999).

[5] *Kalman filter tracking and vertexing in a silicon detector for neutrino physics*, A. Cervera-Villanueva *et al.*. In preparation.